Effect of contact induced states on minimum conductivity in graphene

Roksana Golizadeh-Mojarad and Supriyo Datta
School of Electrical and Computer Engineering, Purdue University, West Lafayette, Indiana 47906, USA
(Received 18 November 2008; revised manuscript received 7 January 2009; published 9 February 2009)

The objective of this paper is to point out that contact induced states can help explain the structure dependence of the minimum conductivity observed experimentally. Contact induced states are similar to the well-known metal induced gap states in metal-semiconductor Schottky junctions, which typically penetrate a few atomic lengths into the semiconductor, while the depth of penetration decreases with increasing band gap. However, in graphene we find that these states penetrate a much longer distance of the order of the width of the contacts. As a result, ballistic graphene samples with a length less than their width at Dirac points can exhibit a length-dependent resistance that is not "Ohmic" in origin but arises from a reduced role of contact induced states. While earlier theoretical works have shown that ballistic graphene samples can exhibit a minimum conductivity, our numerical results demonstrate that this minimum conductivity depends strongly on the structure and configuration of the channel and contacts. In diffusive samples, our results still show that the contact induced states effect needs to be taken into account in explaining minimum conductivity and its dependence on the structure (two terminal vs four terminal) and configuration used.

DOI: 10.1103/PhysRevB.79.085410 PACS number(s): 73.23.Ad, 73.63.−b, 81.05.Uw

I. INTRODUCTION

Recent experiments[1–7] show that the conductivity of graphene (a single atomic layer of graphite) tends to a minimum value in the range of $\sim 2-12\ e^2/h$ as the Fermi energy E_f approaches the charge neutral Dirac points ($E=0$) located at the corners of the Brillouin zone. Around each of these points, the density of states (DOS) is given by $D(E)=E/[\pi(\hbar v_f)^2]$ and the conductivity is expected to approach zero as the Fermi energy E_f approaches zero. Consequently, the experimental observation of a nonzero minimum conductivity has stimulated a lot of theoretical work most of which have focused on the carrier scattering mechanisms in graphene.[8–13] However, a few theoretical works[14–17] have shown that even ballistic graphene samples can exhibit a minimum conductivity and Ref. 18 has considered the role of different shaped contacts. But, all prior works has focused on two-terminal measurements and the purpose of this paper is to point out that the minimum conductivity in ballistic samples depends strongly on the structure (two terminal vs four terminal) and configuration used. We also present the concept of contact induced states whose physics is similar to that of evanescent modes as used in earlier works.[14–18] While samples with dimensions longer than mean-free path are not ballistic and involve scattering processes, our results show that the minimum conductivity due to the contact induced states effect is magnitude wise comparable to the minimum conductivity yielded by scatterers[9] and needs to be taken into account in explaining the minimum conductivity and its structure dependence.

Contact induced states are similar to the well-known metal induced gap states (MIGS) in metal-semiconductor Schottky junctions which typically penetrate only a few atomic lengths into the semiconductor, while the depth of penetration decreases with increasing band gap. However, in graphene we find that these states penetrate a much longer distance of the order of the width W [Fig. 1(a)], which seems reasonable since the graphene acts like a semiconductor with a small band gap that decreases with increasing W. This is just a heuristic argument but it could possibly even be applied to metallic graphene by noting that although the lowest transverse mode has no gap, higher modes do have a width-dependent gap leading to evanescent modes very similar to semiconducting graphene. In this paper, we will present model calculations showing how these contact induced states can help understand many of experimental measurements of minimum conductivity in different multiprobe configurations.

II. MODEL

The basic theoretical model presented here is based on the general nonequilibrium Green's function (NEGF) approach, which has been described elsewhere in detail.[19] The structure is partitioned into channel and contact regions with the channel properties described by a tight-binding Hamiltonian (H) appropriate for graphene with a single π orbital for each carbon atom: all elements of $[H]$ are equal to zero except for nearest neighbors for which $H_{mn}=-t$; $t=2.71$ eV.

The effect of contacts on the channel is included through the self-energy matrix $[\Sigma_{L,R}]$ whose elements are given by $\Sigma_{L,R}=\tau_{L,R}g_{s(L,R)}\tau^{+}_{L,R}$, where τ is the coupling matrix between the contacts and channel and g_s is the surface Green's function for the contact. The surface Green's function at energy E is obtained from the Hamiltonian for the isolated contact (H_{contact}) using the relation,

$$g_s=[(E+i\eta)I-H_{\text{contact}}]^{-1}, \tag{1}$$

which is evaluated using a recursive method making use of the tridiagonal nature of H_{contact}.[20] Typically η is assumed to be an infinitesimal quantity which for graphene contacts would give a vanishing DOS at $E=0$. Instead we use a finite η adjusted to yield a desired nonzero DOS at $E=0$ in the range of $[0.8-2.2]\times 10^{14}/(\text{eV cm}^2)$ corresponding to what we estimate for contact material used.[1–7,21]

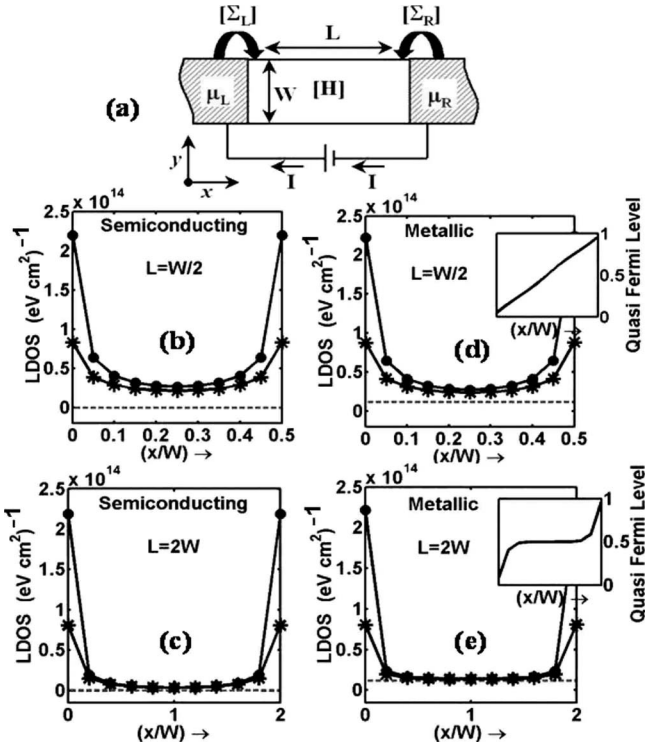

FIG. 1. Effect of contact induced states on an armchair graphene channel in a two-terminal geometry. (a) General schematic illustration used for NEGF quantum transport calculation. Local density of state (LDOS) averaged over the width plotted against the length (x) for (b) semiconducting channel with $L/W=0.5$, (c) semiconducting channel with $L/W=2$, (d) metallic channel with $L/W=0.5$, and (e) metallic channel with $L/W=2$. Dashed line is for when contact DOS is the same as the channel; $*$-line for contact DOS of $8\times10^{13}/(\text{eV cm}^2)$ and ●-line for contact DOS of $22\times10^{13}/(\text{eV cm}^2)$. Also shown in insets is the quasi-Fermi-level profile across the channel normalized to "0" and "1" in the right and left contacts.

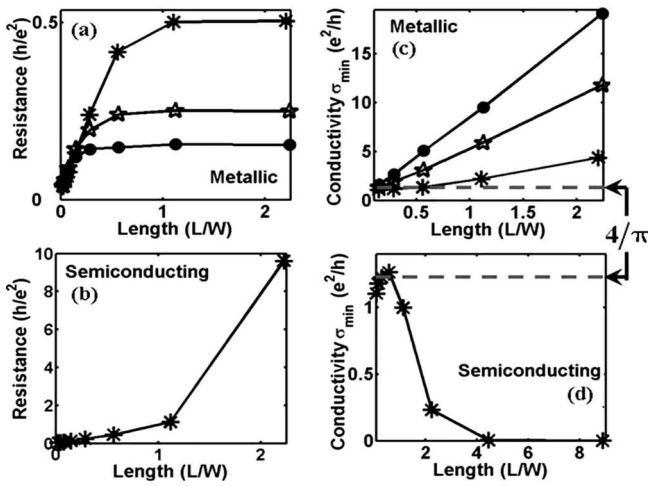

FIG. 2. Effect of the contact induced states on the resistance of a two-terminaled graphene strip. Resistance as a function of the channel length for (a) a metallic armchair channel and (b) a semiconducting armchair channel. Derived conductivity as a function of the channel length for (c) a metallic armchair channel and for (d) a semiconducting armchair channel. $*$-solid line when $T/T_W<0.5$, ★-solid line when $T/T_W\approx3$, and ●-solid line when $T/T_W\approx6$.

III. TWO-TERMINAL GEOMETRY

In order to show the effect of contact induced states on minimum conductivity in graphene, we start with a simple two-terminal geometry for a ballistic armchair ribbon shown in Fig. 1(a). Channels with $L/W<1$ [Figs. 1(b) and 1(d)] show a "punch through" of DOS from one contact to the other, while in channels with $L/W>1$ [Figs. 1(c) and 1(e)] the DOS in the middle approaches the expected value: zero for semiconducting channels and $\sim1/taW$ for metallic channels corresponding to one mode (a: carbon-carbon bond length). Similar results are obtained with zigzag ribbon, except that there are no semiconducting channels, all channels being metallic. Figures 1(c) and 1(e) show that the contact density of states penetrates a distance $\sim W/2$ into the graphene channel.

While contact induced states increase the channel DOS, they decrease the channel resistance. At temperatures low enough that one mode is accessible for metallic channels, for $L/W<0.5$ resistance increases linearly in a manner reminiscent of Ohm's law [Fig. 2(a)], except that this increase is not a result of scattering or momentum relaxation, but from the reduction in *"punch through"* of contact induced states in the channel. Nevertheless, if we extract a sheet conductivity using "Ohm's law" $\sigma=L/RW$, it tends to a constant $(\sim4e^2/\pi h)$ for $L/W<0.5$ and increases linearly as L/W increased [see $*$-line in Fig. 2(c)]. Our numerical results confirm the earlier findings of the theoretical and experimental works for this structure.[14–18,22] These results are not affected significantly by the precise contact density of states for the range of values studied between $[0.8-2.2]\times10^{14}/(\text{eV cm}^2)$. For $L/W>1$ the resistance for metallic channels saturates to $h/2e^2$ corresponding to one spin-degenerate mode [$*$-line in Fig. 2(a)]. More generally, the resistance for long channels saturates to a value R_S that depends on the ratio of the thermal energy k_BT to the energy spacing $kT_W\approx\pi\hbar v_f/4W$ between successive modes. In general $R_S(T/T_W)=h/(e^2\bar{M})$, where the thermally averaged number of modes $\bar{M}=\int dEM(E)(\partial f/\partial E)$ is approximately equal to T/T_W+2 for metallic channels.[23] Figure 2 also shows the calculated resistance and the derived conductivity for values of $T/T_W>1$, indicating the reduction in resistance and enhancement in conductivity expected from the above argument.

Spatial variation in quasi-Fermi level

Insets in Figs. 1(d) and 1(e) show the spatial variation in the quasi-Fermi level for metallic channels. With $L/W=2$, the quasi-Fermi level is flat in the middle of the channel as one would expect for a ballistic conductor. However, near the contacts, it drops sharply. Indeed with $L/W=0.5$ the quasi-Fermi level changes linearly all the way from one contact to the other similar to ordinary diffusive conductors, *although our model includes no scattering*. The linear variation arises

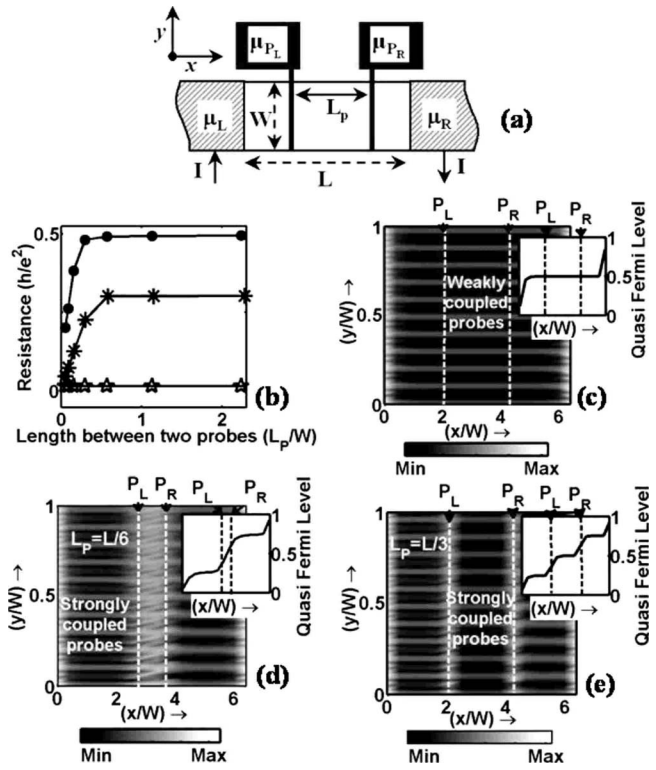

FIG. 3. Effect of contact induced states in Hall bar geometry with full width voltage probes. (a) Schematic illustration of structure. (b) Calculated resistance as a function of the distance between voltage probes (L_P). ★-line for weakly coupled voltage probes; ∗-line for strongly coupled voltage probes with DOS of $22\times10^{13}/(\text{eV cm}^2)$; ●-line for strongly coupled voltage probes with DOS of $8\times10^{13}/(\text{eV cm}^2)$. Two-dimensional (2D) local-density-of-state profile inside a metallic armchair channel for fixed L and W, when (c) the voltage probes are weakly coupled, (d) the voltage probes are strongly coupled for $L_P<W$, and (e) the voltage probes are strongly couple for $L_P>W$. Also shown in insets is the quasi-Fermi-level profile across the channel.

simply from the spatial variation in the DOS. As shown in Ref. 24, the contact resistance between two regions with "M" modes and "N" nodes is proportional to "$1/N-1/M$," so that with spatially varying modes described by $M(x)\sim\hbar v_f D(x)$, we expect a potential profile given by $V(x)\sim -d(D^{-1})/dx$, which is approximately linear as shown [inset Fig. 1(d)].

IV. HALL BAR GEOMETRY

Many experimental measurements employ a four-terminal Hall bar geometry and one might expect from the flat quasi-Fermi level near the middle in inset of Fig. 1(e) that four-terminal measurements would be unaffected by the contact induced state effects we have been discussing. We now present results that while this is indeed true if the voltage probes are "weakly coupled" to the channel ($\tau_{L,R}\approx 0$), strongly coupled voltage probes lead to resistance values that are not too different from what we have been discussing for two-terminal measurements.

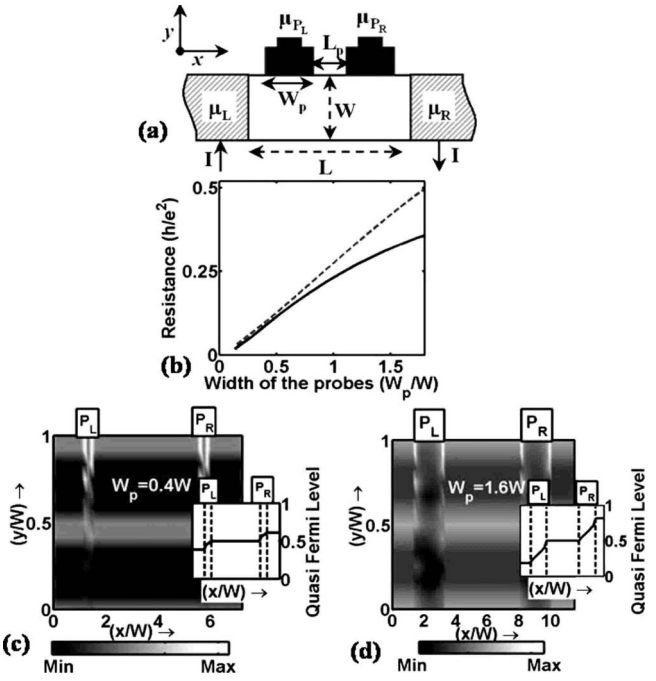

FIG. 4. Effect of contact induced states in four-probe structure with side voltage probes. (a) Schematic illustration of structure. (b) Calculated resistance as a function of width of the side voltage probes (W_P); solid line for contact DOS of $8\times10^{13}/(\text{eV cm}^2)$ and dashed line for contact DOS of $22\times10^{13}/(\text{eV cm}^2)$. 2D local density of state profile inside a metallic armchair channel for fixed L, L_P, and W; (c) $W_P=0.4$ W and (d) $W_P=1.6$ W. Also shown in insets is the quasi-Fermi-level profile across the channel.

A. Full width voltage probes

In this geometry [Fig. 3(a)], if voltage probes are weakly coupled to the channel, they do not induce any states in the channel [Fig. 3(c)]. In this case the calculated resistance [★-line in Fig. 3(b)] is zero since there is no voltage drop deep inside the channel (ballistic regime) as explained above. Experimental voltage probes, however, are strongly coupled leading to a voltage drop between them as shown in Figs. 3(d) and 3(e). The calculated resistance now shows a variation with L_P/W [Fig. 3(b)] similar to the variation in the two-terminal resistance as a function of L/W (Fig. 2). However, with increasing DOS in the probes, we find that the resistance goes down [see ∗-line in Fig. 3(b)] which we ascribe to the increased density of contact induced states in the region between the probes.

B. Side voltage probes

With the voltages probes connected to one side of the channel [Fig. 4(a)], the contact induced states from these probes penetrate along the channel width (y) rather than length (x). If the probe width (W_P) is small compared to the channel width, these probes act like weakly coupled full width voltage probes and the resistance is small [Figs. 4(b) and 4(c)]. The distance between side voltage probes (L_P) does not affect significantly the measured resistance from this geometry since the contact induced state penetration is

along the width of the channel. However wider probes and probes with higher induced density of states cause the probes to affect more of the channel and punch through the width of the channel [Fig. 4(d)] and, hence, measure a higher voltage drop or higher resistance [Fig. 4(b)].

V. COMPARISON WITH EXPERIMENTS

Figure 5 compares the measured minimum conductivities of four-terminal geometries from Ref. 1 with our calculated minimum conductivity for ballistic four-terminal conductors taking contact induced state effects into account. Good agreement is seen for four-terminal measurements (Fig. 5); although several two-terminal measurements from Ref. 1 (not presented here) exceed our predicted conductivity. A possible explanation for these discrepancies is the presence of charged impurities (neglected in this discussion) which have been shown to increase the conductivity.[8,9] This explanation seems supported by the fact that the discrepancies are limited to the samples with the dimensions longer than mean-free path (L_m).

In summary, we have shown that even ballistic graphene samples with $L < W$ at Dirac points can exhibit a length-dependent resistance that is not "Ohmic" in origin but arises from a decreased role of contact induced states. This ballistic model can explain fairly well the experimental results of the devices with the dimensions less than the mean-free path. Finally, contact induced states can account for a number of the experimental observations in both ballistic and diffusive samples such as the structure dependence of minimum conductivity that cannot be explained otherwise.[3]

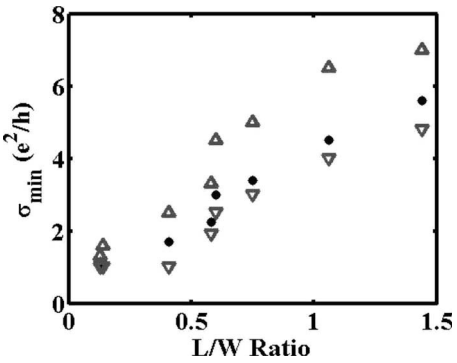

FIG. 5. Comparison between calculated σ_{min} and measured σ_{min} for Hall bar settings of the experiment in Ref. 1. Since the Hall bar geometry used in the experiment is a combination of side probes and probes with widths less than the channel width, we find a range that σ_{min} can fall in for this type of structure considering two limits; side probes [dashed line in Fig. 4(b)] and full probes [$*$-line in Fig. 3(b)]. ●-line: measured σ_{min}; △-line: upper limit of calculated σ_{min}; and ▽ line: lower limit of calculated σ_{min}. We assumed $W_P \sim 250$ nm as estimated from Fig. 1b in Ref. 1. Note that $T/T_W < 0.5$ for the all considered devices.

Note added. Recently, it has come to our attention that a few sets of experiments and theories[25–28] have confirmed some of our predictions.

[1] F. Miao, S. Wijeratne, Y. Zhang, U. C. Coskun, W. Bao, and C. N. Lau, Science **317**, 1530 (2007).
[2] K. S. Novoselov, A. K. Geim, S. V. Morozov, D. Jiang, Y. Zhang, S. V. Dubonos, I. V. Grigorieva, and A. A. Firsov, Science **306**, 666 (2004); K. S. Novoselov, A. K. Geim, S. V. Morozov, D. Jiang, M. I. Katsnelson, I. V. Grigorieva, S. V. Dubonos, and A. A. Firsov, Nature (London) **438**, 197 (2005); Y. Zhang, Y. Tan, H. L. Stormer, and P. Kim, *ibid.* **438**, 201 (2005); A. K. Geim and K. S. Novoselov, Nature Mater. **6**, 183 (2007).
[3] Y. W. Tan, Y. Zhang, K. Bolotin, Y. Zhao, S. Adam, E. H. Hwang, S. Das Sarma, H. L. Stormer, and P. Kim, Phys. Rev. Lett. **99**, 246803 (2007).
[4] J. H. Chen, C. Jang, M. S. Fuhrer, E. D. Williams, and M. Ishigami, Nat. Phys. **4**, 377 (2008).
[5] S. Cho, Y. Chen, and M. S. Fuhrer, Appl. Phys. Lett. **91**, 123105 (2007).
[6] H. B. Heersche, P. Jarillo-Herrero, J. B. Oostinga, L. M. K. Vandersypen, and A. F. Morpurgo, Nature (London) **446**, 56 (2007).
[7] M. Y. Han, B. Ozyilmaz, Y. Zhang, and P. Kim, Phys. Rev. Lett. **98**, 206805 (2007).
[8] K. Nomura and A. H. MacDonald, Phys. Rev. Lett. **98**, 076602 (2007).
[9] Shaffique Adam, E. H. Hwang, V. M. Galitski, and S. Das Sarma, Proc. Natl. Acad. Sci. U.S.A. **104**, 18392 (2007).
[10] V. V. Cheianov, V. I. Fal'ko, B. L. Altshuler, and I. L. Aleiner, Phys. Rev. Lett. **99**, 176801 (2007).
[11] H. Kumazaki and D. S. Hirashima, J. Phys. Soc. Jpn. **75**, 053707 (2006).
[12] T. Ando, J. Phys. Soc. Jpn. **75**, 074716 (2006).
[13] E. H. Hwang, S. Adam, and S. Das Sarma, Phys. Rev. Lett. **98**, 186806 (2007).
[14] M. I. Katsnelson, Eur. Phys. J. B **51**, 157 (2006).
[15] J. Tworzydło, B. Trauzettel, M. Titov, A. Rycerz, and C. W. J. Beenakker, Phys. Rev. Lett. **96**, 246802 (2006).
[16] E. Louis, J. A. Vergés, F. Guinea, and G. Chiappe, Phys. Rev. B **75**, 085440 (2007).
[17] A. Rycerz, Phys. Status Solidi A **205**, 1281 (2008).
[18] H. Schomerus, Phys. Rev. B **76**, 045433 (2007); J. P. Robinson and H. Schomerus, *ibid.* **76**, 115430 (2007).
[19] S. Datta, *Quantum Transport: Atom to Transistor* (Cambridge University Press, Cambridge, 2005).
[20] R. Golizadeh-Mojarad and S. Datta, Phys. Rev. B **75**, 081301(R) (2007).
[21] D. A. Papaconstantopoulos, *Handbook of the Band Structure of Elemental Solids* (Plenum, New York, 1986).
[22] R. Danneau, F. Wu, M. F. Craciun, S. Russo, M. Y. Tomi, J. Salmilehto, A. F. Morpurgo, and P. J. Hakonen, Phys. Rev. Lett. **100**, 196802 (2008).

[23] For metallic graphene channel

$$\frac{\partial f}{\partial E} \approx \frac{1}{4k_B T} e^{-[\pi E/(4k_B T)^2]^2} \quad \text{and} \quad M(E) \approx \frac{WE}{\pi \hbar v_f} + 2.$$

[24] S. Datta, *Electronic Transport in Mesoscopic Systems* (Cambridge University Press, Cambridge, 1997), p. 112.

[25] G. Giovannetti, P. A. Khomyakov, G. Brocks, V. M. Karpan, J. van den Brink, and P. J. Kelly, Phys. Rev. Lett. **101**, 026803 (2008).

[26] E. J. H. Lee, K. Balasubramanian, R. T. Weitz, M. Burghard, and K. Kern, Nat. Nanotechnol. **3**, 486 (2008).

[27] B. Huard, N. Stander, J. A. Sulpizio, and D. Goldhaber-Gordon, Phys. Rev. B **78**, 121402(R) (2008).

[28] P. Blake, R. Yang, S. V. Morozov, F. Schedin, L. A. Ponomarenko, A. A. Zhukov, I. V. Grigorieva, K. S. Novoselov, and A. K. Geim, arXiv:0811.1459 (unpublished).